

# FLOATING POTENTIAL CONSTRAINTS AND FIELD-CIRCUIT COUPLINGS FOR ELECTROSTATIC AND ELECTROKINETIC FINITE ELEMENT MODELS

H. De Gersem<sup>(1)</sup>, R. Belmans<sup>(1)</sup> and K. Hameyer<sup>(1)</sup>

<sup>(1)</sup>Katholieke Universiteit Leuven, Dep. ESAT, Div. ELEN,  
Kasteelpark Arenberg 10, B-3001 Leuven-Heverlee, Belgium

**ABSTRACT.** To retain small models, electrostatic and electrokinetic finite element formulations are linked with several field-circuit couplings and floating potential constraints. The approaches enable convenient simulations of a condenser bushing and a dielectric heating device.

## INTRODUCTION

Finite element discretisations are beneficial for models with complicated geometries, nonlinearities and eddy current effects. Full size finite element models of technical devices, however, often suffer from unacceptably large simulation times. In this paper, only subdomains in which important local effects occur, are discretised by finite elements. Other parts of the device can be modelled up to a sufficient accuracy by appropriate boundary conditions and circuits coupled to the finite element formulation. The resulting hybrid approach is particularly suited for technical modelling and yields small discrete models. The shorter computation times allow the models to be embedded in iterative design procedures and optimisation routines that inevitably incorporate a large number of finite element evaluations.

## FLOATING POTENTIAL CONSTRAINTS

The idea of floating potential constraints is developed for the electrostatic case. The partial differential equation  $-\nabla \cdot (\epsilon \nabla V) = q$  with  $\epsilon$  the permittivity,  $V$  the voltage and  $q$  the charge density, is discretised on the computational domain  $\Omega$  using nodal shape functions  $N_i(x, y, z)$ . The corresponding system of equations is written in tensor notation as

$$k_{ij}u_j = f_i - k_{iq}u_q \quad (1)$$

with  $u_j$  unknown and  $u_q$  known voltages associated with the mesh vertices. The coefficients are

$$k_{ij} = \int_{\Omega} \epsilon \nabla N_i \cdot \nabla N_j d\Omega; \quad f_i = \int_{\Omega} q N_i d\Omega. \quad (2)$$

The boundary of a perfectly electrically conducting region is under static or quasi-static conditions an equipotential surface. The charge is concentrated at the conductor surface. Conductors to which a prescribed voltage is assigned, are explicitly described by Dirichlet boundary conditions by the  $k_{iq}u_q$ -terms. The effect of perfect redistribution of the charge

within conductors at a floating potential, however, is not satisfactorily represented by the finite element model so far.

A perfectly conducting surface  $\Gamma_v$  can be modelled by a *floating potential constraint* [2]. The shape functions associated with the nodes  $s=1,\dots,z$  at the conductor surface are arranged together into one *macro-element* [4] (Figure 1):

$$N_w(x, y, z) = \sum_s N_s(x, y, z) \quad (3)$$

and all individual  $N_s(x, y, z)$  are removed from the original set of shape functions. Single voltage unknowns  $u_w$  are assigned to the degrees of freedom associated with the macro-elements. Within the Galerkin approach, each macro-element serves as a test function as well. The associated equation  $\kappa_{vj}u_j + \kappa_{vw}u_w = I_v - \kappa_{vq}u_q$  with the coefficients defined as in Eq. 2, relates the accumulated charge at the conductor surface to its voltage [1]. Because the floating potential unknown is coupled to the unknowns associated with all nodes adjacent to the conductor surface, this equation is relatively dense. The coupled system of equations is

$$\begin{bmatrix} k_{ij} & k_{iw} \\ k_{vj} & k_{vw} \end{bmatrix} \begin{bmatrix} u_j \\ u_w \end{bmatrix} = \begin{bmatrix} f_i - k_{iq}u_q \\ f_v - k_{vq}u_q \end{bmatrix}. \quad (4)$$

Dirichlet boundary conditions can be interpreted as a floating potential boundary conditions with fixed voltages. Impedance boundary conditions [3] are more general than floating potential boundary conditions in that sense that they relax the perfect conducting property.

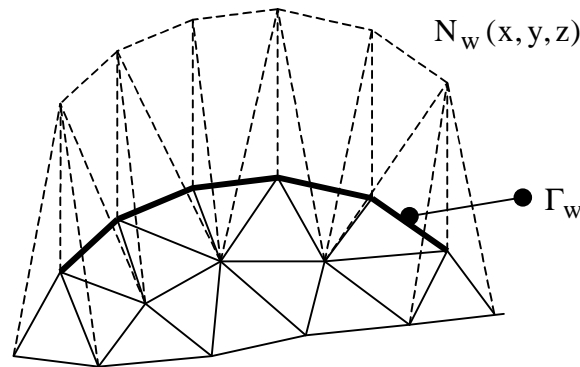


Figure 1. Conductor surface shape function  $N_w(x, y, z)$  built by adding all finite element shape functions defined for the nodes at the conductor surface  $\Gamma_w$ . The surface shape function is 1 at nodes at the surface and vanishes at all other nodes.

## APPLICATION OF FLOATING POTENTIAL CONSTRAINTS

An example of applying floating potential constraints deals with insulators of high-voltage conductors for penetrating grounded walls, floors and metal tanks, called *bushings* [5] (Figure 2). They consist of an insulator, mainly porcelain filled with oil, around the high-voltage conductor. This configuration suffers from locally high electric field strengths that are particularly harmful at the triple junction area. This difficulty is reduced by the conductor bushing principle. A number of concentric conducting cylinders form a series connection of capacitors and redistribute the electric field towards the top of the bushing. Two identical bushings, without and with conducting cylinders (Figure 2), are modelled accounting for their cylinder symmetric geometry. A voltage of 75 kV is applied to the vertical conductor. The bushing is fixed on a transformer tank being at ground potential.

Floating potential boundary conditions are applied to model the equipotential surfaces of the conducting cylinders. To each of the cylinder surfaces, one finite element degree of freedom is assigned. The rather big supports of both macro-elements give rise to two dense equations in the coupled system of equations. The conducting cylinders push the electric field towards the top of the bushing. As a result, the electric field strength diminishes at the junction points. Break-through at this crucial zone is prevented.

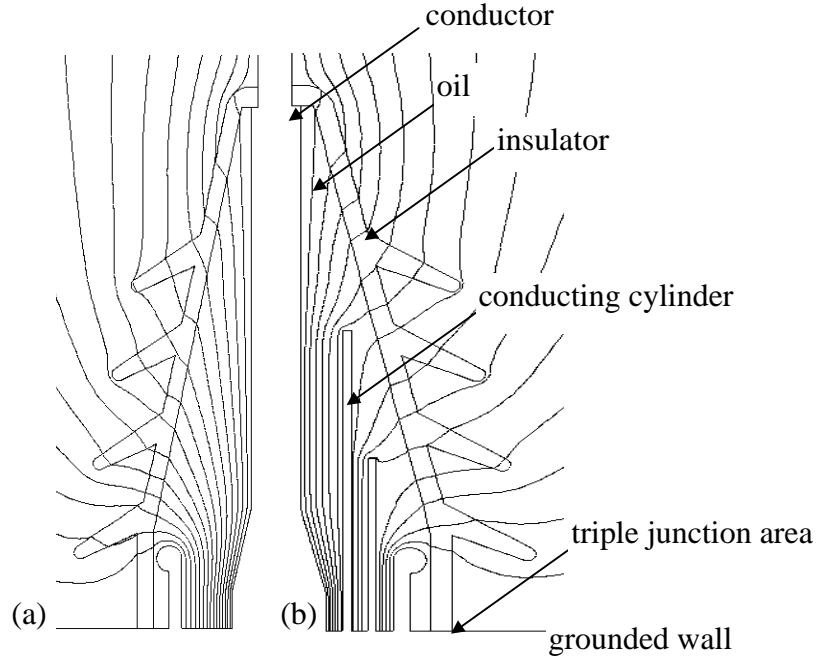


Figure 2. Equipotentials of the voltage in (a) a non-condenser and (b) a condenser bushing.

## EXTERNAL CIRCUITS

Electrokinetic formulations are beneficial for finite element models of induction furnaces and dielectric heating devices. Here, a time-harmonic formulation based on the electric vector potential and the magnetic scalar potential is applied:

$$\nabla \times (\rho \nabla \times \mathbf{T}) + j\omega\mu\mathbf{T} = j\omega\mu\nabla\psi. \quad (5)$$

The electric vector potential  $\mathbf{T}$  is defined by  $\nabla \times \mathbf{T} = \mathbf{J}$  with  $\mathbf{J}$  the current density. The magnetic scalar potential  $\psi$  is related to  $\mathbf{T}$  by  $\nabla\psi = \mathbf{T} - \mathbf{H}$  with  $\mathbf{H}$  the magnetic field strength.  $\rho$  is the resistivity,  $\mu$  the permeability and  $\omega$  the pulsation. In 3D, Eq. 5 is preferably discretised by edge elements. Full 3D models, however, are often unnecessarily large. The geometry of many devices features a translational or cylindrical symmetry. A finite element discretisation of the corresponding cross-section  $\Omega$  may be sufficient to accurately resolve the current paths in the device. In the cartesian case,  $\mathbf{T} = (0, 0, T_z) = (0, 0, \gamma / \ell_z)$  with  $\ell_z$  the length of the model. For cylinder symmetry, the coordinate system  $(r, \theta, z)$  is used and the electric vector potential is  $\mathbf{T} = (0, T_\theta, 0) = (0, \gamma / \alpha r, 0)$ .  $\alpha$  denotes the angular length of the cylinder symmetric model and equals in most cases  $2\pi$ . Where both situations differ from each other, this is indicated by superscripts (cart) or (cyl). In both cases,  $\gamma$  denotes the current between a point  $(x, y, z)$  or  $(r, \theta, z)$  and a reference point at which the constraint  $\mathbf{T} = 0$  is applied. The edge elements  $\mathbf{w}_i = N_i \mathbf{e}_z$  or  $\mathbf{w}_i = N_i \mathbf{e}_\theta$  are introduced. The magnetic voltage drop perpendicular to the subdomain  $\Omega_s$  is defined by  $\Theta_s = -\ell_z \nabla\psi$  or  $\Theta_s = -\alpha r \nabla\psi$ . The discrete form of Eq. 5 reads

$$\tilde{k}_{ij}\gamma_j + \tilde{p}_{is}\Theta_s = -\tilde{k}_{iq}\gamma_q \quad (6)$$

with

$$\tilde{k}_{ij}^{(\text{cart})} = \int_{\Omega} \left( \frac{\rho}{\ell_z} \nabla N_i \cdot \nabla N_j + j\omega \frac{\mu}{\ell_z} N_i N_j \right) dx dy; \quad \tilde{p}_{is}^{(\text{cart})} = \int_{\Omega_s} j\omega \frac{\mu}{\ell_z} N_i dx dy \quad (7)$$

$$\tilde{k}_{ij}^{(\text{cyl})} = \int_{\Omega} \left( \frac{\rho}{\alpha r} \nabla N_i \cdot \nabla N_j + j\omega \frac{\mu}{\alpha r} N_i N_j \right) dr dz; \quad \tilde{p}_{is}^{(\text{cyl})} = \int_{\Omega} j\omega \frac{\mu}{\alpha r} N_i dr dz. \quad (8)$$

The 2D model assumes all  $\Theta_s$  to be known and does not account for more general magnetic coupling of the currents. Moreover, the electrical connections of the model are only represented by the  $-\kappa_{iq}\gamma_q$ -boundary conditions being inconvenient if complicated supply schemes are involved. In this paper, the flux closing paths and external flux sources are modelled by a magnetic circuit external to the finite element model and an additional electric circuit is applied to account for the electrical supply. For numerical reasons, it is recommended to couple the finite element model and both circuit models in one system matrix.

#### Magnetic circuit coupling

For the 2D electrokinetic model, the magnetic flux is perpendicular to the computational domain, in the  $z$ -direction for cartesian, in the  $\theta$ -direction for cylinder symmetric models (Figure 3). The flux linked with the subdomain  $\Omega_s$  is

$$\phi = \int_{\Omega_s} \mu \mathbf{H} \cdot d\mathbf{S} = G_s \Theta_s + \frac{\tilde{p}_{sj}}{j\omega} u_j \quad (9)$$

$G_s$  denotes the DC conductance of the magnetic path through the finite element model:

$$G_s^{(\text{cart})} = \int_{\Omega_s} \frac{\mu}{\ell_z} d\Omega; \quad G_s^{(\text{cyl})} = \int_{\Omega_s} \frac{\mu}{\alpha r} d\Omega \quad (10)$$

The last term in Eq. 9 represents the electromagnetic coupling between currents and fluxes.

The external magnetic equivalent circuit may consist of flux sources  $\phi_{\text{src}}$ , magnetic voltage sources  $\Theta_{\text{src}}$ , reluctances  $R_{\text{ext}}$  and magnetic inductances  $L_{\text{ext}}$  (Figure 3). Magnetic inductances are lumped parameters modelling lossy effects that may exist outside the finite element model, e.g., eddy current losses in ferromagnetic material, electromagnetic shielding or mechanical supports. The circuit model is arranged into a system of equations by choosing an appropriate set of unknowns and deriving their corresponding equations. If no magnetic voltage sources are present in the magnetic circuits, a common modified nodal analysis of the circuit part would be sufficient to obtain a coupled system preserving symmetry and sparsity of the original finite element system matrix. To allow for arbitrary couplings, a more general approach is chosen. The formulation ends up with a mixed description in terms of both unknown magnetic voltages and unknown fluxes.

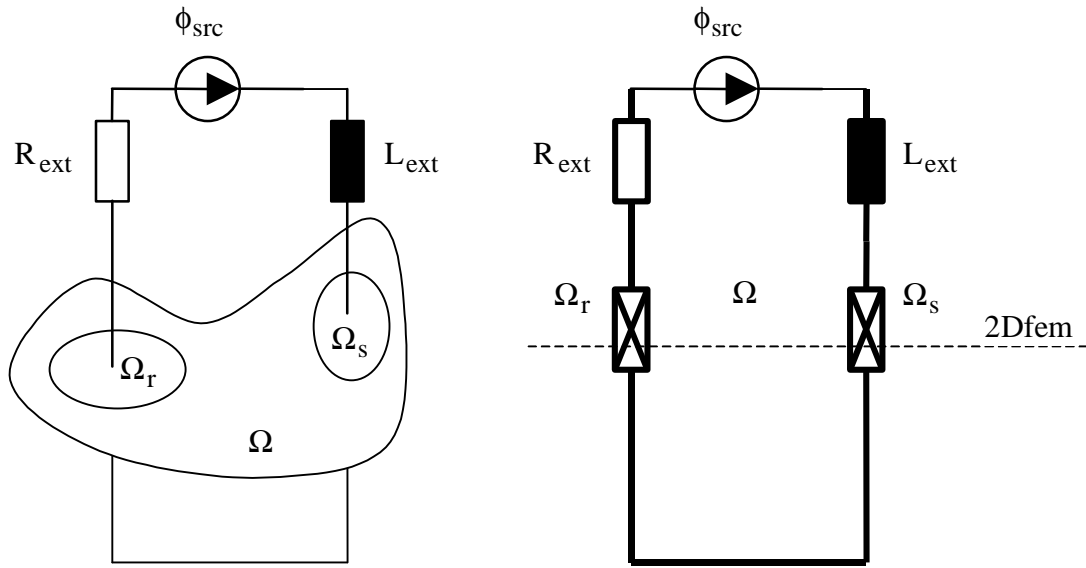


Figure 3. Scheme of the electrokinetic field to magnetic circuit coupling (thin lines indicate links, thick lines tree branches).

A *tree* is a set of branches connecting all circuit nodes without forming loops. Participating branches are selected in order of priority: magnetic voltage sources, branches coupled to the electrokinetic field, reluctances, magnetic inductances and flux sources. The non-selected branches are called *links* and form the *co-tree*. A *cut-set* is a set of branches that by removal would give rise to two distinct circuit parts. Each tree branch can be completed to a *fundamental cut-set* by selecting a number of links. A *loop* is a closed path through the circuit. A *fundamental loop* consists of one link and a set of tree branches. All magnetic voltage and flux sources are supposed to belong to the tree and co-tree respectively. If not, Kirchhoff's voltage law has to be checked for each fundamental loop associated with a magnetic voltage source link and Kirchhoff's current law has to be verified for each fundamental cut-set associated with a flux source tree branch. If the tests fail, the circuit is not solvable, otherwise, the superfluous sources are discarded.

The tree defines a partitioning of the circuit allowing for a convenient formulation of the field-circuit coupled problem. The tree branches and links are indicated by the subscripts "tr" and "ln" respectively. The formulation associates magnetic voltages  $\Theta_{tr}$  to the tree branches and fluxes  $\phi_{ln}$  to the links. For the independent sources, denoted by an additional subscript "&", the values  $\Theta_{tr\&}$  and  $\phi_{ln\&}$  are known in advance. The application of Kirchhoff's laws to the fundamental cut-sets and loops leads to

$$\phi_{tr} + D_{tr,ln}\phi_{ln} + D_{tr,ln\&}\phi_{ln\&} = 0 ; \quad (11)$$

$$\Theta_{ln} + B_{ln,tr}\Theta_{tr} + B_{ln,tr\&}\Theta_{tr\&} = 0 . \quad (12)$$

D and B are fundamental cut-set and loop matrices. They collect the incidences 0, 1 and -1 between the branches of the fundamental cut-sets and loops. It is assumed that all coupled branches are part of the tree. If not, the more elaborated version of this approach described in [7] has to be applied. The priorities applied while tracing the tree ensure that the relations between the magnetic voltages and the fluxes of the individual branches can be written as

$$\phi_{tr} = G_{tr}\Theta_{tr} + g_{tr,j}\gamma_j \quad (13)$$

$$\Theta_{ln} = \Lambda_{ln}\phi_{ln} + j\omega L_{ln}\phi_{ln} \quad (14)$$

Here,  $G_{tr}$  denotes the conductances of the reluctance tree branches and the branches coupled to the electrokinetic finite element model.  $\Lambda_{ln}$  and  $L_{ln}$  represent the reluctances and magnetic inductances of the links. The coupled system of equations is

$$\begin{bmatrix} k_{ij} & p_{i,tr} \\ p_{tr,j} & j\omega G_{tr} & j\omega D_{tr,ln} \\ & -j\omega B_{ln,tr} & -j\omega \Lambda_{ln} + \omega^2 L_{ln} \end{bmatrix} \begin{bmatrix} \gamma_j \\ \Theta_{tr} \\ \phi_{ln} \end{bmatrix} = \begin{bmatrix} f_i - k_{iq} \gamma_q \\ -j\omega D_{tr,ln} \phi_{ln} \\ j\omega B_{ln,tr} \Theta_{tr} \end{bmatrix} \quad (15)$$

The property  $D_{tr,ln} = -B_{ln,tr}^T$  of circuit theory and the application of an appropriate scaling by  $j\omega$  symmetrises the external circuit equations with respect to the finite element equations. Also, the coupling mechanism preserves the sparsity of the original finite element system.

### Electric circuit coupling

For many technical devices, the supply and the load can not be simulated independently from each other. For some parts of the electric model, e.g. the electric supply and the resonating circuit, a circuit model is sufficiently accurate whereas, in most cases, the load requires a much finer discretisation. The boundary of the electrokinetic finite element model in Figure 4a consists of three *current walls*,  $\Gamma_0$ ,  $\Gamma_1$  and  $\Gamma_2$ , and three *current gates*  $\Xi_0$ ,  $\Xi_1$  and  $\Xi_2$ . The uniqueness of the electric vector potential solution is ensured by setting the potential zero at one reference current wall per connected finite element domain ( $\Gamma_0$  in Figure 4a).

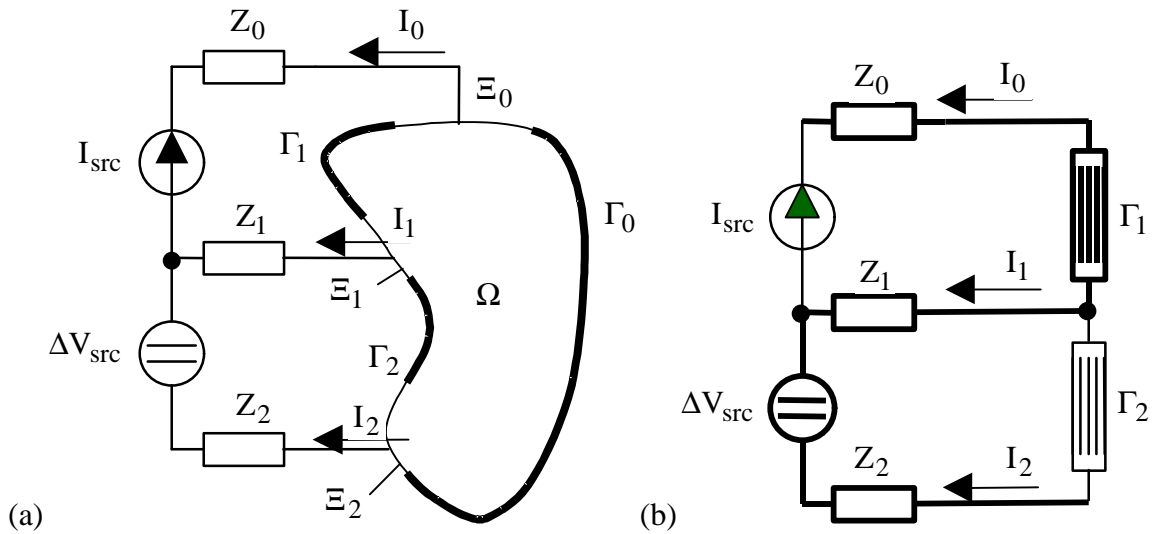


Figure 4. Electrokinetic finite element model coupled to an electrical circuit (thin lines indicate links, thick lines tree branches).

The current leaving the finite element domain  $\Omega$  through the current gate  $\Xi_v$  is

$$I_v = \gamma_{v+1} - \gamma_v \quad (16)$$

Each of the current walls except the reference current wall, is represented by an electric conductor in the external magnetic circuit (Figure 4b). To each electric conductor, the current  $I_v = \gamma_v$  is assigned. Eq. 16 is then automatically satisfied by circuit topology. A surface shape function is associated with each current wall (Figure 1). Hence, each current wall  $I_v$

behaves as a floating potential boundary with the unknown potential  $\gamma_v$ . Within the Galerkin weighted residual approach, the flux wall shape functions except the one associated with the reference wall, are added to the set of test functions. The weak formulation of Eq. 5 corresponding to the test function  $N_v$  is

$$\tilde{k}_{vj}\gamma_j + \tilde{k}_{vw}\gamma_w - \int_{\partial\Omega} N_v \rho \nabla \gamma \cdot \mathbf{d}\Gamma = \tilde{f}_v \quad (17)$$

The boundary integral term satisfies

$$- \int_{\partial\Omega} N_v \rho \nabla \gamma \cdot \mathbf{d}\Gamma = - \int_{\Gamma_v} \mathbf{E} \cdot \mathbf{d}\Gamma = \Delta V_v \quad (18)$$

with  $\Delta V_v$  the voltage drop between two successive current gates  $\Xi_{v-1}$  and  $\Xi_v$ .

The currents through the current gates are related to the electric vector potentials at the current walls. The treatment of the remaining part of the circuit is similar as in the previous section. The fundamental loop and cut-set matrices  $\mathbf{B}_{ln,tr}$ ,  $\mathbf{B}_{ln,tr\&}$ ,  $\mathbf{D}_{tr,ln}$  and  $\mathbf{D}_{tr,ln\&}$  are built. Unknown voltage drops  $\Delta V_{tr}$  are assigned to the independent tree branches and unknown currents  $I_{ln}$  to the independent links. The Kirchhoff current and voltage laws are expressed for the corresponding fundamental cut-sets and loops. The coupled system of equations is

$$\begin{bmatrix} \tilde{k}_{ij} & \tilde{k}_{iw} & & & & \\ \tilde{k}_{vj} & \tilde{k}_{vw} & & & & \\ & & Y_{tr} & & & \\ & & -\tilde{\mathbf{B}}_{ln,w} & -\tilde{\mathbf{B}}_{ln,tr} & & \\ & & & & -Z_{ln} & \end{bmatrix} \begin{bmatrix} \gamma_j \\ \gamma_w \\ \Delta V_{tr} \\ I_{ln} \end{bmatrix} = \begin{bmatrix} \tilde{f}_i - \tilde{k}_{iq}\gamma_q \\ \tilde{f}_v - \tilde{k}_{vq}\gamma_q \\ -\tilde{\mathbf{D}}_{tr,ln\&} I_{ln\&} \\ \tilde{\mathbf{B}}_{ln,tr\&} \Delta V_{tr\&} \end{bmatrix} \quad (19)$$

with  $Y_{tr}$  and  $Z_{ln}$  the admittances and impedances of the tree branches and the links.

## APPLICATION OF EXTERNAL CIRCUIT COUPLING

A dielectric heating device is considered as an example [9] (Figure 5). A cylindrical dielectricum is placed between two circular electrodes. Both dielectric and conductive heating effects are considered. The combination of conductive and dielectric effects involves a complex-valued resistivity

$$\underline{\rho} = \frac{1}{\sigma + j\omega\epsilon} \quad (20)$$

in Eq. 5. If the geometrical dimensions exceed the wave length, wave phenomena are observed. Geometry and excitation allow for an axisymmetric model. The magnetic circuit applies the short-circuit connection of all magnetic paths. The heating device is excited by an electric circuit containing a voltage source, a resistor and a resonant circuit.

## CONCLUSIONS

Floating potential constraints and field-circuit couplings enable efficient finite element models for electrotechnical devices. The models of a condenser bushing and a dielectric heater focus on the application of these techniques to electrostatic and electrokinetic formulations.

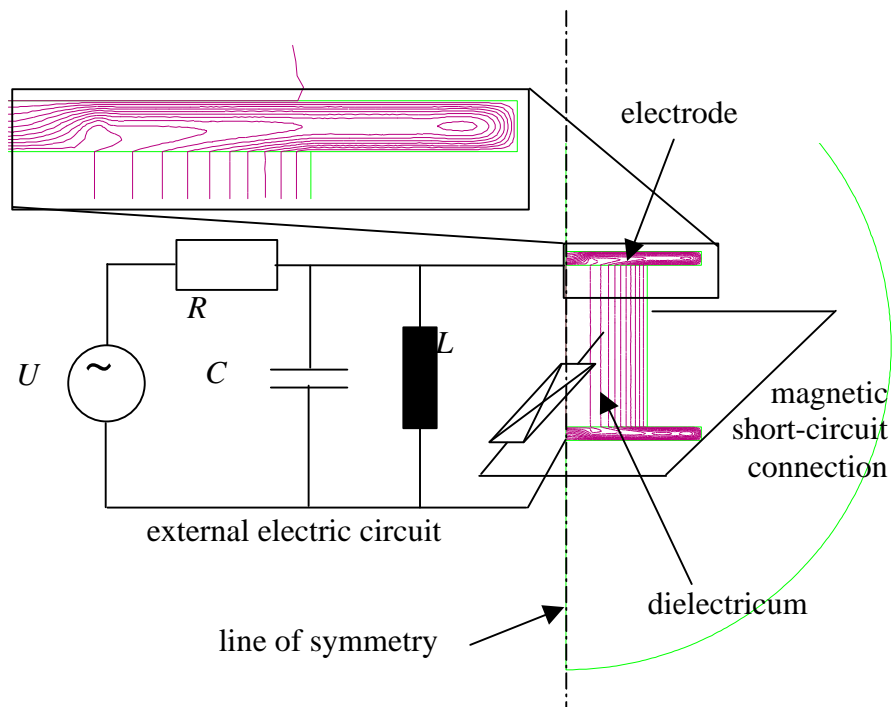


Figure 5. Cylinder symmetric electrokinetic finite element model of a dielectric heating device coupled to an external magnetic and electric circuit.

#### ACKNOWLEDGEMENT

The authors are grateful to the Belgian “Fonds voor Wetenschappelijk Onderzoek - Vlaanderen” (project G.0427) and the Belgian Ministry of Scientific Research (project IUAP No. P4/20 on Coupled Problems in Electromagnetic Systems) for the financial support of this work. The Research Council of the K.U.Leuven supports the basic numerical research.

#### REFERENCES

- [1] Dular, P., Legros, W., Nicolet, A. (1998). Coupling of local and global quantities in various finite element formulations and its application to electrostatics, magnetostatics and magnetodynamics. *IEEE Transactions on Magnetics*, 34-5, 3078-3081.
- [2] Konrad, A., Graovac, M. (1995). The finite element modelling of conductors and floating potentials. *IEEE Transactions on Magnetics*, 32-5, 4329-4331.
- [3] Gyimesi, M., Lavers, D. (1994). Impedance boundary condition for multiply connected domains with exterior circuit conditions. *IEEE Transactions on Magnetics*, 30-5, 3056-3059.
- [4] Dular, P., Legros, W., De Gersem, H., Hameyer, K. (1998). Floating potentials in various electromagnetic problems using the finite element method. *Proceedings of the 4th International Workshop on Electric and Magnetic Fields*, Marseille, France 1998, 409-414.
- [5] Roth, A. (1965). *Hochspannungstechnik*. Springer-Verlag, Wien.
- [6] De Gersem, H., Hameyer, K. (2000). Electrodynamics finite element model coupled to a magnetic equivalent circuit. *European Physical Journal Applied Physics*, 12-2, 105-108.
- [7] De Gersem, H., Mertens, R., Pahner, U., Belmans R., Hameyer, K. (1998). A topological approach used for field-circuit coupling. *IEEE Transactions on Magnetics*, 34-5, 3190-3193.
- [8] Philips, D.A. (1992). Coupling finite elements and magnetic networks in magnetostatics. *International Journal for Numerical Methods in Engineering*, 35, 1991-2002.
- [9] Metaxas, A.C. (1996). *Foundations of Electroheat: a unified approach*. Wiley, Chichester.